

## **ANALYSIS OF EXCESSIVE HEATING ON THE THERMAL AND ELECTRICAL RESISTANCE OF A POLYMER ELECTROLYTE MEMBRANE FUEL CELL**

**W. A. N. W. Mohamed and R. Atan**

Alternative Energy Research Centre (AERC)  
Faculty of Mechanical Engineering, Universiti Teknologi MARA  
40450 Shah Alam, MALAYSIA  
E-mail: wanjerm3@yahoo.com.my

### **ABSTRACT**

The performance on a polymer electrolyte membrane (PEM) fuel cell is evaluated based on the relationship of thermal and electrical resistances to its electrical and thermal power output. An analytical method by which the electrical resistance is evaluated based on the polarisation curve and the thermal resistance from the mass balance, was applied to a 72-cell PEM fuel cell assembly. In order to evaluate the effect of resistances at elevated stack temperatures, the cooling system was operated at half of its maximum cooling effectiveness. The increase in current and resistance due to a unit change in temperature at a particular density was evaluated and it was found that the stack has a ratio of thermal resistance rise to current rise of 1.7, or equal to 0.00584 A/W of current increase per stack heat increase. These values suggest that the internal resistance of the stack components, most probably the electrode assemblies, are very high, which should be addressed in order to obtain lower resistances to current flow.

**Keywords:** PEM, fuel cell, thermal, electrical resistance.

### **INTRODUCTION**

In a world where pollution is an immediate threat to the quality of life, fuel cell systems are viewed with increasing seriousness as a leading solution in many alternative energy considerations. A fuel cell turns the chemical energy within a hydrogen-based-fuel into electricity using oxygen (air) and other catalysts, through a series of electrochemical reactions. The fuel cell generates useful electrical energy without any polluting emissions; the by-products are typically just heat and water. As a remarkably efficient, incredibly clean source of energy, fuel cells can replace both batteries and engines to power vehicles, power national supply grids and all sorts of other stationary and mobile applications. Current research trends in fuel cell technology cover both fundamental, as well as high-tech applications. General research areas include: the development of constituent materials, cell design, processing and manufacturing, multi-scale modelling and simulation, performance reliability, stack design and configurations, power electronics, cost optimisation, practical applications, fuel sources and thermal management or thermal engineering (Sopian and Daud, 2006).

Thermal management has been widely acknowledged as an important area in ensuring high cell performance and efficiency (Faghri and Guo, 2005). It relates directly to the power output performance of the cells within the system as well as cell life. The

generation of electrical power within the fuel cell system also generates a near-equivalent amount of heat energy, which means the higher the power produced, the greater the heat released. At elevated cell temperatures, the stability of power density is affected, due to the higher membrane resistance to proton flow as the membrane dehydrates, which reduces the overall efficiency of the system. Therefore, the cells require continuous cooling, by either air or water cooling systems. For low temperature, compact and mobile capability operations, the hydrogen proton exchange membrane fuel cell (PEMFC), also known as polymer electrolyte membrane, is widely applied. The main criterion of a PEMFC is that the electrolyte is an ion-conducting polymer membrane and when combined with the anode and cathode on both sides of the membrane, is known as the membrane electrode assembly (MEA).

PEMFCs operate at a lower temperature than other fuel cell types; typically in the range of 50 to 80 °C. This gives the advantage of a faster startup time but the heat produced would be of low grade (Dhathathreyan and Rajalakshmi, 2007). It can also operate over a wide range of pressures. PEMFC stacks are also modular and simple to construct. The normal load for a PEMFC application is in the range of 0.1 W to 100 kW, making it very attractive over a wide range of engineering applications. The operation of a PEMFC involves electrochemical reactions at microscopic levels. Hydrogen flows through one side of the membrane and is catalytically split by an oxidation half-cell reaction to form protons and electrons (Figure 1). This reaction occurs at a layer called the Gas Diffusion Layer (GDL) by using platinum-based electrodes as the anode. The protons are permitted to travel through the membrane to the cathode side. The formation of H<sub>2</sub>O and the internal resistance of the electrical circuit releases heat as the direct product of the reactions in the PEMFC. The heat concentration is normally higher at the cathode side, increasing the cell temperature and causing membrane dehydration if the heat is not effectively removed (Al-Baghdadi and Al-Janabi, 2007).

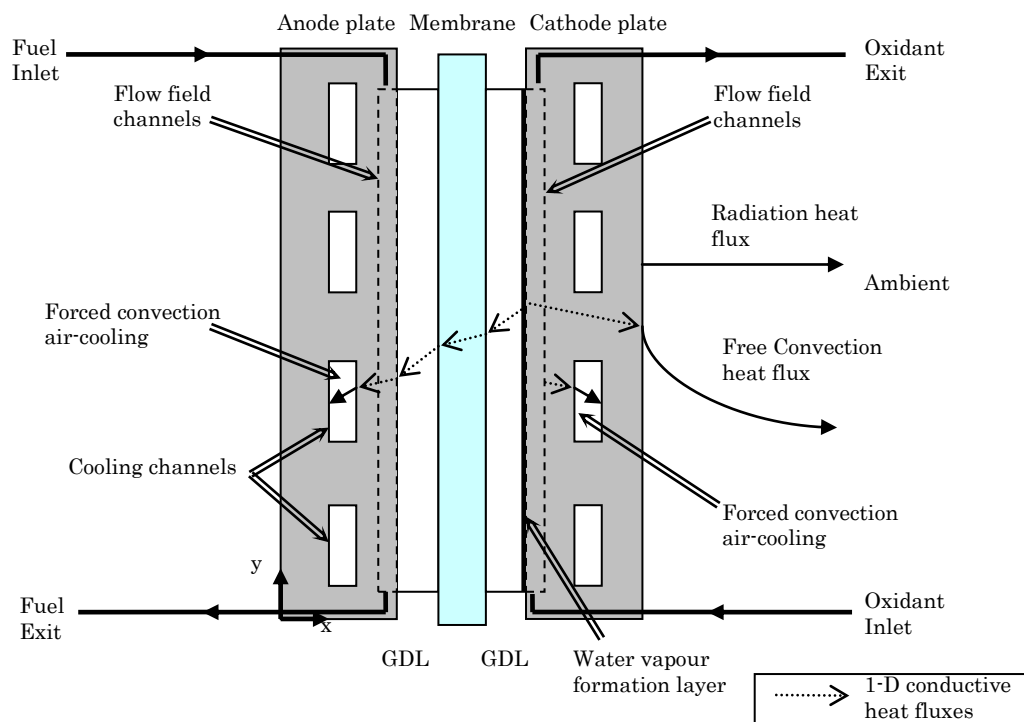


Figure 1. Single cell PEMFC operation with relation to thermal characteristics.

The power generation of a PEMFC is a function of many process parameters and stack temperature plays an important role in power generation stability. Researchers have identified the effect of stack temperature on the electrical power, such as Graf et al. (2006), who explains that even a slight increase in stack temperature would cause an increase in generated current. However, the voltage across the stack would drop significantly as stack temperature increases. The efficiency of a typical PEMFC is 40% to 50%, meaning that about half of the energy produced dissipates as other forms of energy, mainly heat. The loss in electrochemical performance is due to irreversibility of the cathodic reaction, to ohmic resistance and mass transport over potentials. Heat removal should be adequate to prevent the membrane drying and a rise in cell temperature. Normally, in a heat transfer study, thermal resistance refers to the flow of heat generated within a medium. Within this study, thermal resistance is the factor of thermal heat generated at a fixed voltage and current value. High thermal resistance indicates that more energy is lost as heat than converted to useful electrical power.

Internal electrical resistance, also known as ohmic losses, is due to the losses during ionic and charge transport. The cell components that contribute to electrical resistance are: the electrolyte, the catalyst layer, the gas diffusion layer, bipolar plates, interface contacts and the terminal connections. The term ohmic loss in a fuel cell study refers to the reduction of voltage by internal resistance to ionic and charge transport. Because ionic transport through the membrane is more difficult than electronic charge transport via the plated and cell terminals, the resistance posed by the electrode and electrolyte is significantly higher. The key to reducing ionic resistance is to maintain the humidity of the membrane at the required levels, which is directly related to thermal management issues. Identifying the parameters affecting a stack operation is an important aspect of continuous improvement in the design process. Works on the effects of cell temperature (Jang et al., 2007), water content (Park and Caton, 2008), flow field designs (Li et al., 2007 and Wang et al., 2008), are some of the attempts to relate fuel cell performance to its design and operating conditions. An analytical approach (Pandiyan et al., 2008) based on empirical data to determine the thermal and electrical resistances of a stack, related directly to the stack heat generated during operation, is referred to in this work. It is very useful to characterise the internal resistance changes occurring within a fuel cell as a tool for performance evaluation. The works presented here applied the analysis on a 72-cell stack arrangement with limited cooling, as a tool to investigate the effects of internal resistances to the power output, as the stack is heated in excess and operated beyond its designated operating temperature.

## MODEL AND FORMULATION

The electrical power supplied to the load is evaluated using:

$$P_{electrical} = V \times I \quad (1)$$

Heat generation occurs mainly at the cathode from the electrochemical formation of water and from the electron and proton flows (ohmic resistance). The stack thermal energy was evaluated from temperature changes of the stack, added together with the heat removed from the stack via active and passive cooling calculations, to cater for the ohmic resistance heat generation. Thus, the stack heat energy is slightly higher than the theoretical electrochemical heat generation.

$$P_{thermal} = Q_{stack} + Q_{active\ cooling} + Q_{passive\ cooling} \quad (2)$$

The stack heat change over a unit time is given by:

$$\frac{\Delta Q_{stack}}{\Delta t} = m_{stack} \cdot C_{stack} \Delta T_{stack} \quad (3)$$

where:  $m$  is the mass of the stack,  $C$  refers to the specific heat of the stack (homogeneous assumption) and  $\Delta T$  is the experimental stack temperature change over a period of time.

The quantifiable heat removed by the active cooling and passive cooling, respectively, is given by:

$$Q_{active} = Q_{coolant} = \dot{m} C_p \Delta T \quad (4)$$

$$Q_{passive} = Q_{nat-conv} + Q_{radiation} \quad (5)$$

where:  $\dot{m}$  is the mass flow rate of the cooling water,  $C_p$  is the specific heat of water at constant pressure and  $\Delta T$  is the coolant temperature difference between the inlet and outlet of the stack.

The heat generated by the stack is related to the total thermal resistance of the components within the stack assembly. Thermal resistances of a substance are normally designated based on the temperature change over a unit of thermal power, or K/W. Pandiyan et al. (2008) suggested that the total stack energy generated and the stack thermal resistance, can be related to the current flow by expressing it as:

$$P_{thermal} = Q_{stack} = I^2 / R_{thermal} \quad (6)$$

Thus, the thermal and electrical resistances in units of ohms can be calculated from the respective equations:

$$R_{thermal} = P_{th} / I^2 \quad (7)$$

$$R_{electrical} = V / I \quad (8)$$

By combining Eqs (7) and (8), the following equations were developed to evaluate the rise in current and the rise in resistance, due to each unit of cooling water temperature change.

$$I_1^2 R_1 = \dot{m}_{cw} C_p \Delta T_1 \quad (9)$$

$$I_2^2 R_2 = \dot{m}_{cw} C_p \Delta T_2 \quad (10)$$

$$\dot{m}_{cw} C_p (\Delta T_2 - \Delta T_1) = (I_2^2 - I_1^2)(R_1 - R_2) \quad (11)$$

## EXPERIMENTAL DETAILS

The experiment was conducted using a water-cooled 72-cell PEM fuel cell system. The system configuration, schematic and general specifications of the hardware are presented in Figure 2, Figure 3 and Table 1, respectively. The stack and system was designed by a fuel cell design and manufacturing company based in Singapore, which is known to be the only one in South-East Asia. The major working fluids involved in fuel cell operation are the reactants of hydrogen and air, plus the cooling mediums of water and air. Table 2 summarises the operating conditions of the experiment. The measurements were taken at 3 minutes intervals using a thermal scanner and K-type thermocouples with a data logger for local temperatures at 18 designated points of the stack, an anemometer for air velocity and a multi-meter for electrical power measurement at the resistant loader. In order to evaluate the effect of thermal and electrical resistances at stack temperatures higher than the designated 50 °C operating temperature, the cooling water circulation was limited to half, giving a calculated cooling effectiveness of 40% to 50% during fuel cell operation. The experiment was stopped when the average stack temperature reached 70 °C as a higher temperature could cause permanent damage to other system components.



Figure 2. PEM fuel cell system with thermal measurement probe arrangement.

Table 1. PEM fuel cell system specifications.

Specification	Information / Details
Max power output rating	3 kW at 48V
Number of cells	72
Operating temperature	50 °C
Cell size (bipolar plate)	150 mm length, 240 mm height, 5 mm thick
Cooling system	Water-cooled with heat exchanger

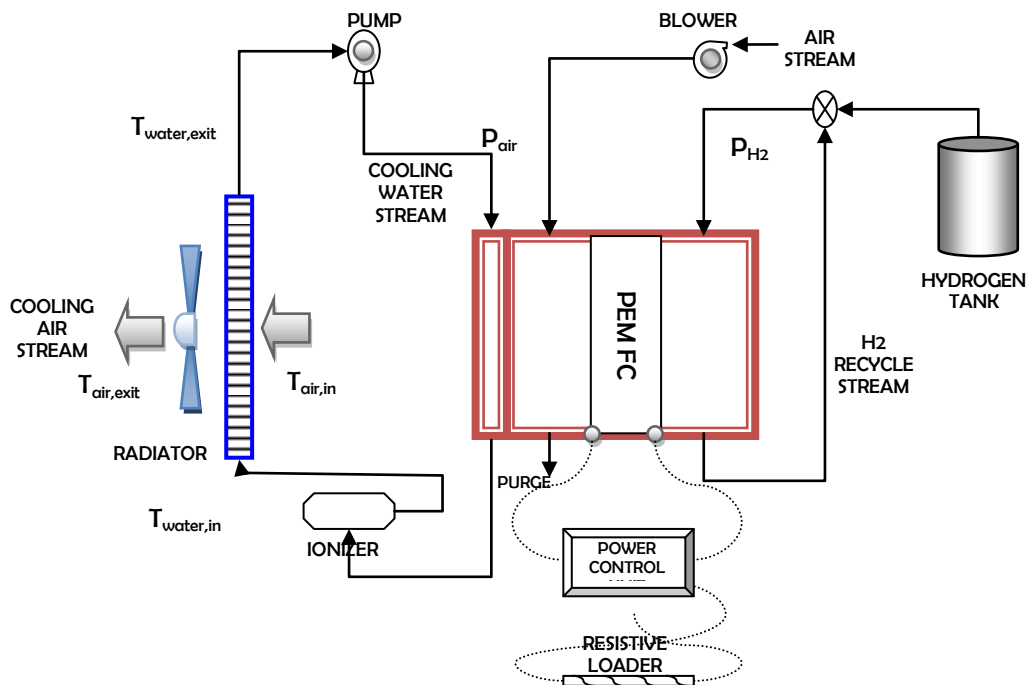


Figure 3. The fuel cell system schematic.

## RESULTS AND DISCUSSION

The electrical resistive loader draws current from the fuel cell stack at a nearly uniform value of 11 to 13.5 A (refer to Figure 4). The corresponding voltage was between 33 to 27.7 V. A decrease in power output was observed as the stack operates, with maximum power and minimum power outputs of 440 and 320 W, respectively. The decline in power output and current density was related to the average stack temperature (refer to Figures 5 and 6). The average power decline was 7.6 W/°C or 1% from the maximum value and the cell conversion efficiency reduced at a near linear rate of 0.11% per degree Celsius of stack temperature rise. The humidity levels of the membrane allowed a peak power output when the stack temperature was 39 °C. The cell current density reduced significantly when the stack temperature was between 39 to 57 °C as the membrane dehydrates and increased proton resistance occurs. The power and current density stabilises at higher temperatures, showing that energy and charge transport equilibrium was achieved within the cells.

Table 2. Operating conditions.

<b>PEM Fuel Cell stack</b>	
<b>Properties / parameters</b>	<b>Values</b>
1. Material	Carbon graphite
2. Specific heat, $C$ (Begot and Kaufmann, 2008)	710 J/kg.K
3. Density	2240 kg/m <sup>3</sup>
4. Stack volume	0.010557 m <sup>3</sup>
5. Top surface area	0.05775 m <sup>2</sup>
6. Side surface areas	0.1848 m <sup>2</sup>
7. Thermal conductivity (Dumercy et al., 2006)	20 W/m.K
8. Surface emissivity (Cengel, 2003)	0.85
9. Conversion efficiency	45%
<b>Reactants</b>	
1. Hydrogen inlet pressure	1.5 bar
2. Air inlet pressure	1 bar
<b>Cooling Water</b>	
1. Operating pressure	1 atm
2. Specific heat, $C_p$	4180 J/kg.K
3. Mass flow rate	0.0126 kg/s
<b>Cooling Air</b>	
1. Inlet temperature	≈ 26 °C
2. Inlet pressure	1 atm
3. Specific heat, $C_p$	1007 J/kg.K
4. Mass flow rate	0.065274 kg/s
5. Density	1.174 kg/m <sup>3</sup>

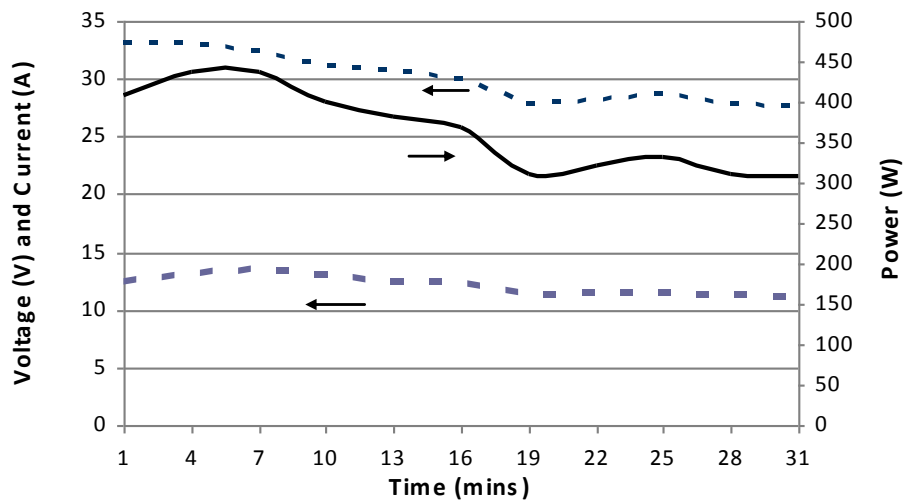


Figure 4. The stack voltage, current and electrical power profile over operation time.

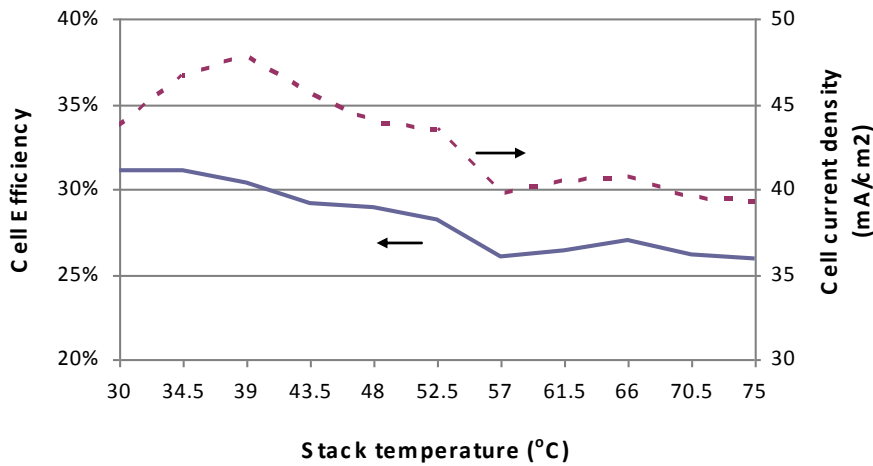


Figure 5. Relation of cell efficiency and current density to average stack temperature.

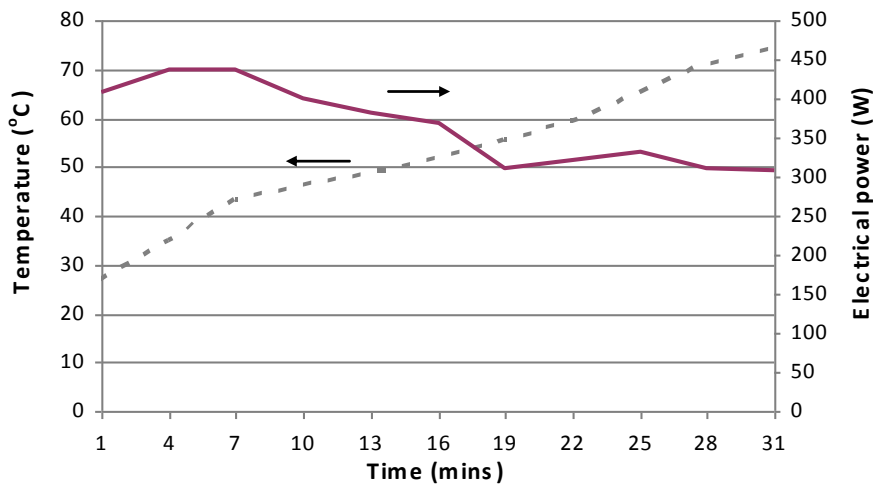


Figure 6. Time-based stack temperature and power output profile.

The rapid rise of stack heat was due to the low active cooling contribution set for the study, which was calculated at 40% to 50% heat exchanger effectiveness. If a linear relationship is assumed, then the stack heat increase rate is approximately 113 W/min. The actual stack heat from Figure 7 is in the range of 750 to 2030 W and the maximum value was registered as the stack temperature crossed 70 °C.

Experimental data shows that the stack thermal power at 1000 W corresponds to a cooling water temperature change of 19 °C, a stack current of 12.41 A and a total voltage of 30.8 V. These values form the basis of calculations from Eq. (9) and Eq. (10) for two cases of theoretical and actual rise of current and resistances. Table 3 lists the current and resistance value based on the theoretical linear stack thermal power rise of 50 W per degree change in cooling water temperature. The actual current and resistance changes were evaluated by interpolating the experimental data of current, voltage and thermal power generated for a similar trend in cooling water unit temperature change. Figure 8 graphically presents the theoretical and experimental current and resistance changes.

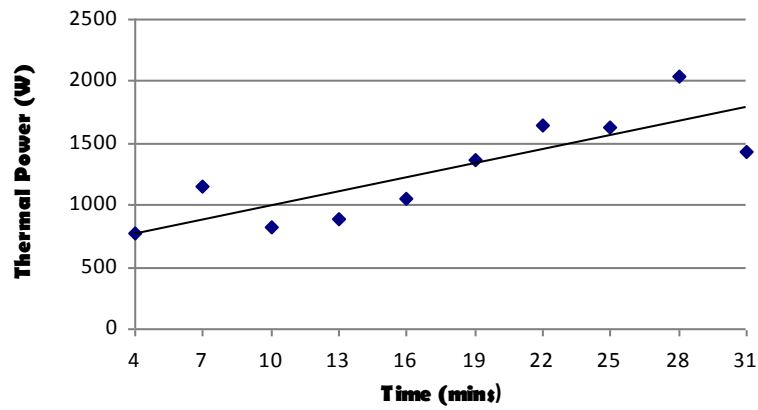


Figure 7. Quantitative stack thermal energy.

Table 3. Theoretical case of stack current and resistance changes.

Theoretical stack thermal power (W)	CW temperature change ( $\Delta T$ )	Current (Amps)	Thermal resistance (ohms)	Electrical resistance (ohms)
1000	0	12.41	6.50	2.48
1050	1	12.73	6.84	2.42
1100	2	13.05	7.18	2.36
1150	3	13.35	7.52	2.31
1200	4	13.65	7.87	2.26
1250	5	13.95	8.21	2.21
1300	6	14.24	8.55	2.16
1350	7	14.52	8.89	2.12
1400	8	14.79	9.23	2.08
1450	9	15.07	9.58	2.04
1500	10	15.33	9.92	2.01

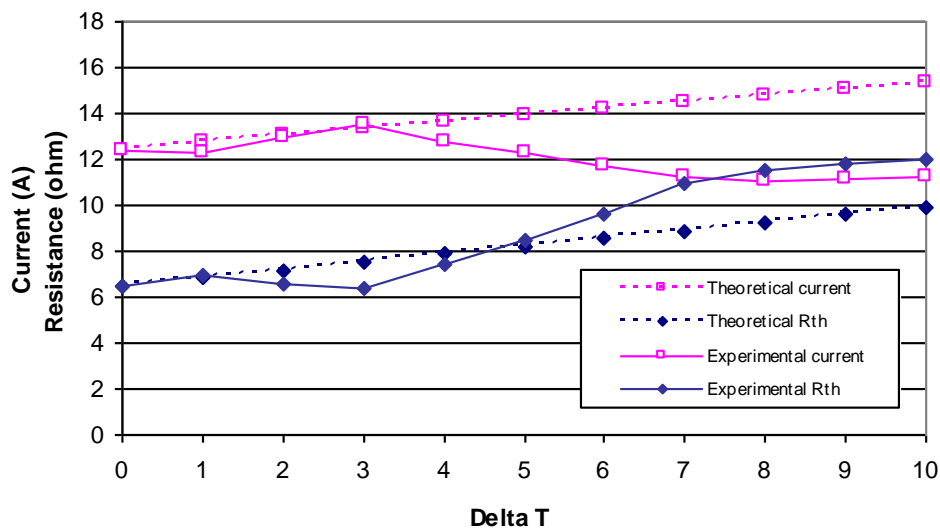


Figure 8. Current and thermal resistance changes for a unit change of temperature.

The theoretical thermal resistance increases by 50% for a temperature difference of 10 °C, whereas the current increases by only 30%. The current increase rate is 0.292 A/°C of cooling water temperature increase, or 0.00584 A/W of stack heat increase. The current rise is due to the slightly lower electrical resistance as the stack temperature increases. A large current rise is subdued due to increasing thermal resistance. Theoretically, the ratio of thermal resistance rise to the current rise is 1.7. Referring to the works of Pandiyan et al. (2008), the same ratio for their 4-cell assembly is 3 with a current change rate of 1.76 A/°C of cooling water temperature increase, or 0.13 A/W of stack heat increase. The stack in this study registers a 70% lower current change rate compared to the 4-cell stack, pointing to higher internal resistance within the stack assembly. Pandiyan et al. (2008) highlighted that the electrode fabrication procedure is a major contributor to high internal resistance of fuel cell stacks. Another possible reason is damaged cells within the stack that contribute to higher electrical resistance and consequently, act as a thermal generator. Figure 9 compares the theoretical and experimental electrical resistance of the stack. The theoretical resistance reduces as the stack heats up, as the electron charge transport receives external energy and the bipolar plate structure expands. The experimental electrical resistance declined at a lower rate than the theoretical resistance until  $\Delta T = 3$  °C. Then, a surge on a magnitude of 0.3 ohms was registered at  $\Delta T = 4$  °C and the consequent electrical resistance hovered in the range of 2.48 to 2.51 ohms, when theoretically it should be declining, suggesting that one or more cells were already damaged.

Overall, the comparison of theoretical with experimental data for a 10 °C rise of cooling water temperature indicates a contradictive trend. Theoretical analysis predicts a 30% increase in electrical current when the thermal resistance increases by 50% and the electrical resistance decreases by 20%. However, actual data plots indicate a decline of electrical current by 8% as the thermal resistance increases to 100% at a near constant electrical resistance value. In this case, the experimental values demonstrate a behaviour that is too sensitive to actual operating conditions, mainly to the cell conditions (reduced humidity due to over-heating, mass flow and concentration etc.). The general correlation between the experimental and theoretical resistance values, applicable to all PEM fuel cell stacks, is an area that certainly requires further studies.

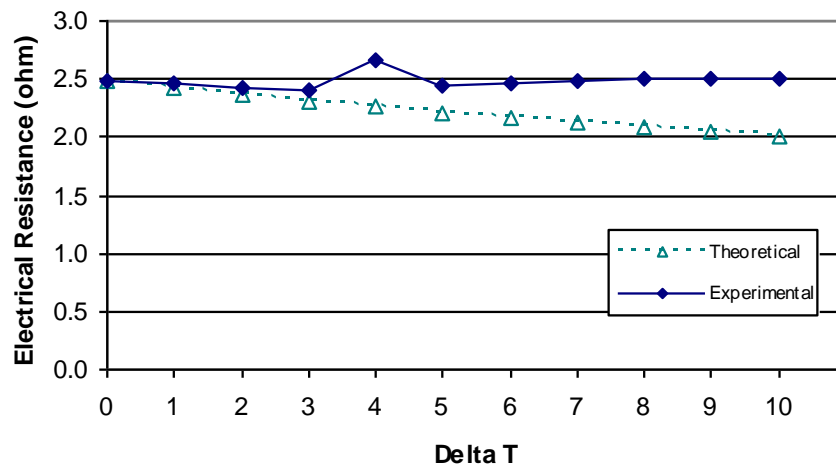


Figure 9. Comparison of theoretical with experimental electrical resistance change.

## CONCLUSIONS

Fuel cell performance is affected by the state of each of its components as well as its operating conditions. An analytical investigation based on the influence of internal resistance was carried out on a PEM fuel cell stack constrained with limited cooling. Thermal and electrical resistance of a PEM fuel cell stack was empirically measured based on Ohms law. The total thermal power of the fuel cell was found to have significant influence on the current output. The current rise to a unit of stack heat increase was very low, suggesting the influence of internal resistance, which may arise from electrode quality or cells damaged during operation. The analytical method presented has successfully enabled a fuel cell performance analysis from the perspective of power to resistance relations, which can be applied to compare the performance of different stacks. However, a definite mathematical relationship between the resistances based on actual performance data would require further work in this area.

## REFERENCES

- Faghri, A. and Guo, Z. 2005. Challenges and opportunities of thermal management issues related to fuel cell technology and modelling. *International Journal of Heat and Mass Transfer*, 48 (19-20): 3891-3920.
- Begot, S. and Kauffmann J.M. 2008. Estimation of internal fuel cell temperatures from surface temperature measurements. *Journal of Power Sources*, 178(1): 316-322.
- Cengel, Y.A. 2003. *Heat transfer: A practical approach Int. Edition*. New York: McGraw Hills.
- Dhathathreyan, K.S. and Rajalakshmi, N. 2007. Polymer electrolyte membrane fuel cell, recent trends in fuel cell science and technology. *Sudshawatsu B. (Eds.)*. India: Anamaya Publications.
- Dumercy, L., Glises, R., Louahlia-Gualous, H. and Kaufmann, J.M. 2006. Thermal management of a PEMFC stack by 3D nodal modelling. *Journal of Power Sources*, 156(1): 78-84.
- Graf, C., Vath, A. and Nicoloso, N. 2006. Modeling of the heat transfer in a portable PEFC system within MATLAB-Simulink. *Journal of Power Sources*, 155(1): 52-59.
- Jang, J.H., Chiu, H.C., Yan, W.M. and Sun, W.L. 2007. Effects of operating conditions on the performances of individual cell and stack of PEM fuel cell. *Journal of Power Sources*, 180(1): 476-483.
- Al-Baghdadi, M.A.R.S. and Al-Janabi, H.A.K.S. 2007. Modeling optimizes PEM fuel cell performance using three-dimensional multi-phase computational fluid dynamics model. *Energy Conversion and Management*, 48(12): 3102-3119.
- Pandiyani, S., Jayakumar, K., Rajalakshmi N. and Dhathathreyan, K.S. 2008. Thermal and electrical energy management in a PEMFC stack-an analytical approach. *International Journal of Heat and Mass Transfer*, 51(3-4): 469-473.
- Park, Y.H. and Caton, J.A. 2008. Development of a PEM stack and performance analysis including the effects of water content and cooling method. *Journal of Power Sources*, 179: 584-591.
- Sopian, K. and Daud, W.R.W. 2006. Challenges and future developments in Proton exchange membrane fuel cells. *Renewable Energy*, 31(5): 719-727.

- Wang, X.D., Duan, Y.Y., Yan, W.M. and Peng, X.F. 2008. Local transport phenomena and cell performance of PEM fuel cells with various serpentine flow field designs. *J Power Sources*, 175(1): 397-407.
- Li, X., Sabir, I. and Park, J. 2007. A flow channel design procedure for effective water channel removal. *Journal of Power Sources*, 163(2): 933-942.